Seventh International Conference on Computational Fluid Dynamics (ICCFD7), Big Island, Hawaii, July 9-13, 2012

ICCFD7-2706

Evaluation of Numerical Dissipation Sensitivity Using IDDES

Zhixiang Xiao*, Jian Liu*,**, Kunyu Luo* and Song Fu*
Corresponding author: xiaotigerzhx@tsinghua.edu.cn

* School of Aerospace, Tsinghua University, Beijing, China
** China Aerodynamics Research & Development Center, Mianyang, Sichuan, China.

Abstract: Improved-Delayed Detached Eddy Simulation **(**IDDES) method based on two equation k-ω-SST (shear layer transport) model is applied to simulate the decay of homogeneous isotropic turbulence (DHIT) and massive separation flows past tandem cylinders (TC) flows with space of 3.7 diameters (D). Fourth order Jameson-type central scheme (C4) and high order symmetric total variation diminishing (STVD) scheme with adaptive dissipation are formulated by introducing a function (ϕ) dependent on the turbulent flow. The numerical dissipation sensitivity is evaluated by changing the threshold of the function (ϕ_{min}). For the DHIT case, the large ϕ_{min} suppresses the cascade of the energy and the very small ϕ_{min} can match the measurements well; both C4 and STVD schemes have the same tendency. For the TC case, the primary differences of computations are caused by the fundamental schemes, while ϕ_{min} has a relatively weak influence. Due to a small background artificial viscosity coefficient $k^{(4)}$ of 1/100 in C4 scheme, undesired small ϕ (<1) region before the front cylinder is presented, which leads to the appearance of the numerical noise in the near-field around TC; The performance of S6WENO5 is better and anticipant. The shear layer instability happens a little more upstream and structures are smaller with smaller ϕ_{min}.

Keywords: IDDES, DHIT, TC, adaptive dissipation, threshold of the function ϕ_{min}

1 Introduction

Detached eddy simulation (DES) was originally developed to accurately simulate the massively separated flows (Spalart et al., 1997). Due to its high accuracy and efficiency, it was widely used and obtained further improvements. To avoid the undesired transition from RANS (Reynolds-averaged Navier-Stokes) to LES (large eddy simulation) in the attached boundary layer induced by the locally clustered grids, Menter et al. (2003) and Spalart et al. (2006) proposed DDES based on two-equation SST model and one-equation model SA model, respectively. To cure the log-layer mismatch problem, Shur et el. (2008) proposed IDDES, which combines the advantage of DDES and wall-modeled LES (WMLES). In our previous work (Xiao et al., 2011), the performances of three advanced DES methods, such as DDES-2003, 2006 and IDDES, were compared through simulating the massively separated flows past TC case. It's found that the major difference between DDES-2003 and DDES-2006 is the shielding function, which leads to the different range of RANS region. Due to the WMLES mode, IDDES performs better for the shear layer instability and root mean square of pressure coefficient. Then, IDDES is chosen as the turbulence simulation model to predict the

extremely unsteady and massively separated flow past TC in this article. In our previous work about the massive separation around rudimentary landing gear [Xiao et al, 2012], IDDES performs better than DDES on the surface flow patterns, such as the range of horseshoe vortex, secondary separation, and so on.

The natural choice for the numerical scheme of LES and LES/RANS hybrid approaches is the central-type schemes. However, the purely central schemes often suffer from the numerical instability, because the grids near the wall and in the irrotational region are not fine enough to fully resolve the turbulence. Therefore, in these regions, the appropriate numerical dissipation is also required. More and more people have realized the deficiency of the upwind discretization scheme and made very good efforts in eliminating the negative effect of the numerical dissipation to provide accurate results. Three types of efforts can be classified as: (1) increasing the discretization order of the scheme; (2) reducing the numerical dissipation; (3) both.

Bui (1999) directly reduced the dissipation of upwind Roe scheme with 3rd monotone upstream-central schemes for conservation laws (MUSCL) interpolation by multiplying a small constant, ranging from 0.03 to 0.05, to calculate the fully developed turbulence in a square duct with LES. Qin and Xia (2008) reduced the numerical dissipation of Roe scheme in the same way to predict the synthetic jet flow. To obtain the balance of numerical accuracy and stability, the relatively large constant is taken as 0.4. This approach is very simple and easily to implement, but it is too empirical and lacks physics.

The combination of the central and upwind scheme (Strelets, 2001; Mockett, 2009) was smartly designed to accurately predict the turbulence. This upwind/central hybrid scheme functions acts as an effectively central scheme in the separated regions where DES is operating in an LES mode, and as an upwind-biased scheme near the wall (RANS mode) and in the outer irrotational regions.

In our previous work, Xiao et al. (2012) investigated the numerical dissipation effect on the massively separated flows past TC using original upwind Roe scheme with MUSCL interpolation, S6WENO5 (6th order symmetric scheme with 5th order weighted essential non-oscillating interpolation) scheme with 12% dissipation and S6WENO5 scheme with adaptive dissipation (Strelets, 2001), coupled with DDES methods. It's found that the original Roe scheme is too dissipative. It over-predicts the root mean square of pressure coefficients and greatly suppresses the generation of the small-scale structures. S6WENO5 scheme with 12% dissipation performs much better than the original Roe scheme. Unfortunately, it is too empirical. S6WENO5 scheme with adaptive dissipation performs best and it can well predict the mean and instantaneous flows.

Spalart et al. (2012) investigated the unsteady flow and noise from the landing gear using 4th central and 3rd upwind Roe hybrid scheme with three thresholds of adaptive function (ϕ_{min}) of 0, 0.2 and 0.4, respectively. When the more upwind-biased differencing is used, the small-scale contents are greatly reduced. The performance is greatly affected by different ϕ_{min}, which is highly undesirable.

In this article, the threshold of adaptive function (ϕ_{min}) of numerical dissipation is evaluated based on two schemes, 4th order Jameson type central (C4) scheme only with 4th artificial viscosity and S6WENO5 scheme. To obtain reasonable results, the values of ϕ_{min} are less than 0.1. At the same time, the effects of the fundamental schemes on the flow features, such as turbulence energy cascade, shear layer instability, pressure fluctuations, turbulent kinetic energy (TKE) and so on, are explored through comparing with the available measurements.

2 Spatical Schemes and Adaptive Dissipation

The in-house code of UNITs (*U*nseady *N*av*I*er-S*T*okes solver), which is in a cell-centered finite-volume formulation based on multi-block structured grids, is applied to evaluate the numerical dissipation sensitivity. A modified fully implicit LU-SGS with Newton-like sub-iteration in pseudo time is taken as the time marching method when solving the N-S and the turbulence model equations. The approach is a parallel algorithm using domain-decomposition and message-passing-interface strategies for the platform on computer clusters.

In this paper, two high order schemes are used. One is the Jameson-type (1981) C4 scheme and the other is S6WENO5 scheme (2002). The reason for choosing the STVD scheme is that this algorithm allows the independent control of the dispersion and dissipation errors in the solution.

According to our experience, the original Jameson-type central and STVD scheme are often dissipative and they can greatly suppress the generation of small structures. Then, their dissipation should be effectively decreased in the separation region. As was analyzed before, the numerical dissipation should be large enough near the wall and in the irrotational region where the grid are relatively too coarse to accurately resolve the turbulence. The adaptive function, dependent on the flow and grid scale, can be introduced in the convective terms of N-S equations.

The invicid flux of N-S equations can be written as:

$$F_{i+1/2}=f_{i+1/2}+ D_{i+1/2} \tag{1}$$

In equation (1), $f_{i+1/2}$ is the symmetric or central flux and $D_{i+1/2}$ is the pure dissipation.

For the S6WENO5 scheme,

$$f_{i+1/2}=(F_{i-2}-8F_{i-1}+37F_i+37F_{i+1}-8F_{i+2}+F_{i+3})/60 \tag{2}$$

$$D_{i+1/2} = -0.5\times\phi\times\left[\left|\tilde{A}_{inv}\right|\left(q^R - q^L\right)\right]_{i+1/2} \tag{3}$$

where q^R and q^L are the original variables on the right and left side of the interface. In Equation (2), the symmetric scheme is 6^{th} order; in equation (3), the original variables are obtained through 5^{th} WENO interpolation.

For the C4 scheme, only the fourth artificial viscosity remains due to low speed flow. The symmetric flux and dissipation are given as:

$$f_{i+1/2}=(-F_{i-1}+7F_i+7F_{i+1}-F_{i+2})/12 \tag{4}$$

$$D_{i+1/2} = D^{(4)}_{i+1/2} = -\lambda_{i+1/2}\varepsilon^{(4)}_{i+1/2}\left(q_{i+2}-3q_{i+1}+3q_i-q_{i-1}\right), \varepsilon^{(4)}_{i+1/2}=Max(0,\phi\times k^{(4)}) \tag{5}$$

where 4^{th} background artificial viscosity coefficients $k^{(4)}$ is taken as 1/100; λ is the spectral radius and q are the primary variables.

In equation (3) and (5), ϕ is an adaptive function dependent on the turbulence flow and grid scale. It can be written as:

$$\phi=\phi_{max}\tanh(A^{CH1}) \tag{6}$$

where ϕ_{max} is always taken as 1. It means that ϕ theoretically ranges from 0 to 1. The definition of ϕ can be found in our previous work (Xiao et al., 2012) or some other references (Strelets, 2001; Mockett, 2009 and Spalart, 2012). Then, ϕ is designed to be 0 in the separation regions and to become 1 near wall and in irrotational regions. When it is equal to 0, the S6WENO5 scheme becomes the sixth order symmetric scheme without dissipation and C4 scheme is a pure central scheme without any artificial viscosity. When it is equal to 1, it returns to the original scheme.

As we know, high order purely central schemes always suffer from numerical difficulty, and then we should set a threshold of the adaptive function, ϕ_{min}. Then the final adaptive function can be written as:

$$\phi=\max(\phi, \phi_{min}) \tag{7}$$

where ϕ_{min} is a constant, which can be taken as 0.01, 0.1, even 1. To ensure numerical accuracy, it is hoped to be as small as possible.

3 Turbulence Simulation Methods

Differing from the original DES (Spalart et al., 1997), DDES (Spalart et al, 2006) and IDDES (Shur et al., 2008), the background turbulence model in this article is not taken as one-equation S-A model (Spalart, 1992), but two-equation SST model (Menter, 1994). IDDES methods could be constructed by modifying the destruction term of the TKE equation and by introducing a length scale, L_{hybrid}

$$\frac{\partial(\rho k)}{\partial t}+\frac{\partial(\rho u_j k)}{\partial x_j}=\frac{\partial}{\partial x_j}\left(\left(\mu+\frac{\mu_t}{\sigma_k}\right)\frac{\partial k}{\partial x_j}\right)+\tau_{ij}S_{ij}-\frac{\rho k^{3/2}}{L_{hybrid}} \tag{8}$$

For IDDES, the length scale of L_{hybrid} can be written as

$$L_{hybrid}=L_{IDDES}=\tilde{f}_d(1+f_e)\times L_{RANS}+(1-\tilde{f}_d)\times L_{LES} \tag{9}$$

where the length scale of L_{RANS} is defined as $k^{0.5}/(\beta^*\omega)$ and L_{LES} is defined as $C_{DES}\times\Delta$, where $\Delta=\max(\Delta x, \Delta y, \Delta z)$. For IDDES, the grid scale is redefined as $\Delta=\min[\max(C_w\Delta_{max}; C_wD_w; \Delta_{min})$;

Δ_{max}]. When f_e is equal to 0, $L_{IDDES}=\tilde{f}_d \times L_{RANS}+(1-\tilde{f}_d)\times L_{LES}$ and it acts in DDES mode. Function $\tilde{f}_d$ is defined as max[$(1-f_{dt})$; f_B]. It is determined by both the geometry part f_B and the flow part $(1-f_{dt})$. When f_e is larger than zero and $\tilde{f}_d$ is equal to f_B, $L_{IDDES}=L_{WMLES}=f_B(1+f_e)\times L_{RANS}+(1-f_B)\times L_{LES}$, and it acts in WMLES mode.

4 Results and Discussions

The turbulence modeling method is the IDDES based on SST model. The constant C_{DES} has been calibrated using UNITs (Xiao et al., 2012). In this paper, we focus on evaluating the effects of threshold of adaptive function (ϕ_{min}) on the flow features, such as energy cascade, mean pressure, mean velocity, instantaneous shear layer instability, pressure fluctuation, and so on.

4.1 Decay of Homogenous Isotropic Turbulence

DHIT is a fundamental test case for the development of turbulence modeling and/or numerical techniques as it is the simplest realization of the turbulent flow. On the one hand, the capability and quality of LES part in IDDES can be evaluated. On the other hand, the empirical parameter C_{DES} can be recalibrated. At the same time, the dissipation level of the present in-house CFD code can be evaluated. To obtain more resolved turbulence, the dissipation level of numerical scheme should be reduced effectively wherever LES is activated.

The computational domain contains 32^3 uniform cells. The computation of DHIT is established in a cubic domain with periodic boundary conditions in all three directions to reflect the homogeneity of the flow.The temporal scheme is the implicit LU-SGS method with very small non-dimensional time step (0.0001 here).

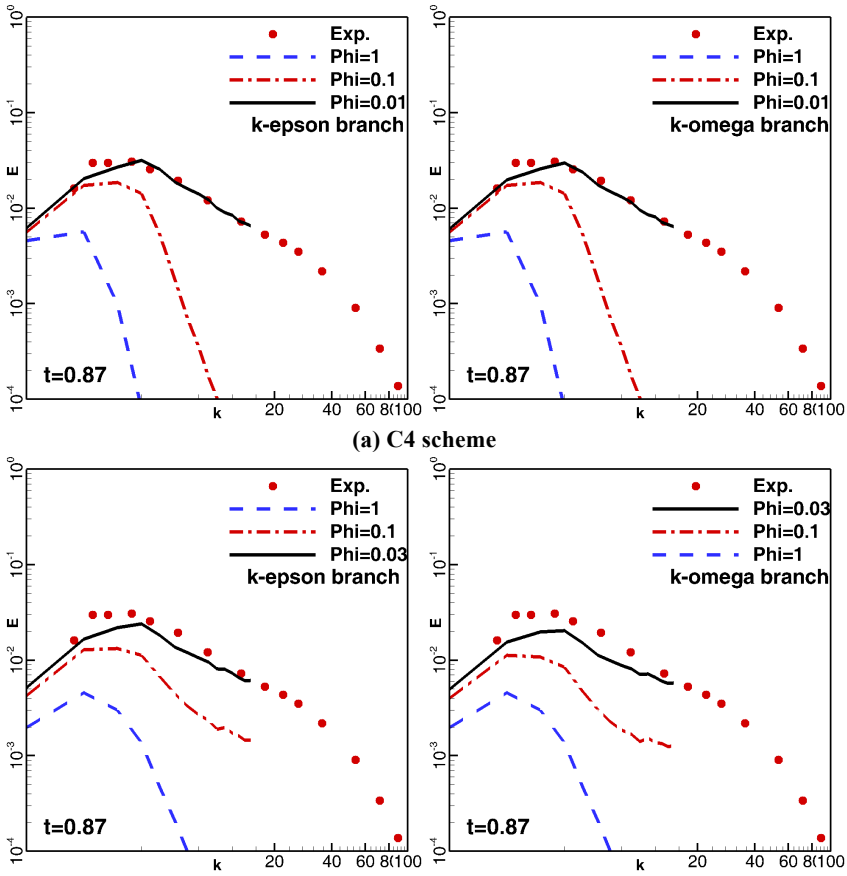

(a) C4 scheme

(b) S6WENO5 scheme

Figure 1: The effects of ϕ_{min} on energy spectra of DHIT.

Like Menter's SST model, IDDES based on SST model also contains k-ω and k-ε branches. For the

DHIT, the k-ε branch is more important because there is no wall in the computational domain.
Figure 1 presents the energy cascade by C4 and S6WENO5 schemes, respectively. For the DHIT case, ϕ is a constant and it is equal to ϕ_{min}. When ϕ is equal to 1, the spatial scheme is the original C4 and S6WENO5 schemes. When ϕ is equal to 0, the spatial scheme becomes the 4^{th} or 6^{th} order central scheme.

(1) For the C4 scheme: The original scheme, where ϕ=1 and $k^{(4)}$=1/100, greatly under-predicts the energy cascade for the all wave numbers. When ϕ is reduced to 0.1, where $k^{(4)}$ =1/1000, it only under-predicts the energy at high-wave numbers. When ϕ is equal to 0.01, where $k^{(4)}$ is equal to 1/10000, it can well predict the energy at both the low- and high-wave numbers. This indicates that 1/10000 of $k^{(4)}$ is an appropriate parameter of ϕ_{min}. The performances of k-ε and k-ω parts differ little.

(2) For the S6WENO5 scheme: The original STVD scheme, where ϕ=1, greatly under-predicts the energy cascade for all the wave numbers. When ϕ is reduced to 0.1, it also under-predicts the energy, especially at high wave number. When ϕ is taken as 0.03, the scheme can well predict the energy at both low and high wave numbers. It indicates that 0.03 is a good choice of ϕ_{min} when S6WENO5 scheme is applied. The energy of k-ε part is a little larger than that of k-ω part using the same ϕ.

In fact, the computations for the complex unsteady flows based on the non-uniform grids often suffer numerical difficulties if the ϕ_{min} value recommended by DHIT case is applied. The actual ϕ_{min} is usually adjusted to a little larger value.

4.2 Tandem Cylinders

The TC case studied here is the one investigated experimentally by Jenkins et al. (2005, 2006 and 2009). It is known to associate with complex flow phenomena, like the transition, separation of turbulent boundary layer, shear layer instability, the interaction of unsteady wake of the front cylinder with the downstream one and unsteady massively separated flow between the cylinders and in the wake of the rear cylinder, and so on. Thus, it is a standard test case in the European 7^{th} Framework project Advanced Turbulence Simulation for Aerodynamic Application Challenges (ATAAC) (2009-2012) and AIAA Workshop on Benchmark problems for Airframe Noise Computations (BANC I and II, 2010, 2012).
The diameters (D) of the two cylinders are the same. The spacing L is 3.7D. The velocity of freestream is 44m/s, the Reynolds number based on D is 1.66×10^5 and the angle of attack is 0 degree. In order to resolve the small-scale structures, the two-dimensional grids between the cylinders are almost isotropic (about 0.01-0.02 D). The spanwise domain is taken as 3D with equal intervals of 0.02D. The overall cells are 12.4 million for the three-dimensional computational domain. The non-dimensional time step is 0.01.
In the present simulations, no-slip conditions are imposed on the cylinders' walls. Symmetric conditions are applied on the lateral sides of the wind-tunnel test-section and periodic conditions are taken in the spanwise direction. At inflow and outflow boundaries, the one-dimensional Riemann characteristic analysis is employed to construct a non-reflection boundary condition. "Ghost cells" are employed to treat all kinds of boundary conditions including the boundaries of the adjacent zonal domains.
As mentioned before, the computations usually suffer numerical difficulties if ϕ_{min} is too small, especially when using the C4 scheme. To ensure the computations on going, ϕ_{min} in C4 scheme are taken as 0.05 and 0.1. For S6WENO5 scheme, ϕ_{min} is taken as 0.03 and 0.1.

4.2.1 Histories of Drag Coefficient (C_d)

Figure 2 presents the histories of C_d on the front and rear cylinders by C4 and S6WENO5 with different ϕ_{min}. From it, the C_d fluctuation amplitude of the front cylinder is significantly smaller than that of the rear one. It means that the flow past the front cylinder seems relatively "quiet". This feature is easily understood as the front cylinder encounters weaker disturbances of the free-stream than the rear one, which is in the extremely unsteady wake detached from the front cylinder.

After averaging the instantaneous drag coefficients (C_d), the mean C_d coefficients are listed in Table 1. The difference is mainly caused by the fundamental schemes and different ϕ_{min} have a relatively weak influence.

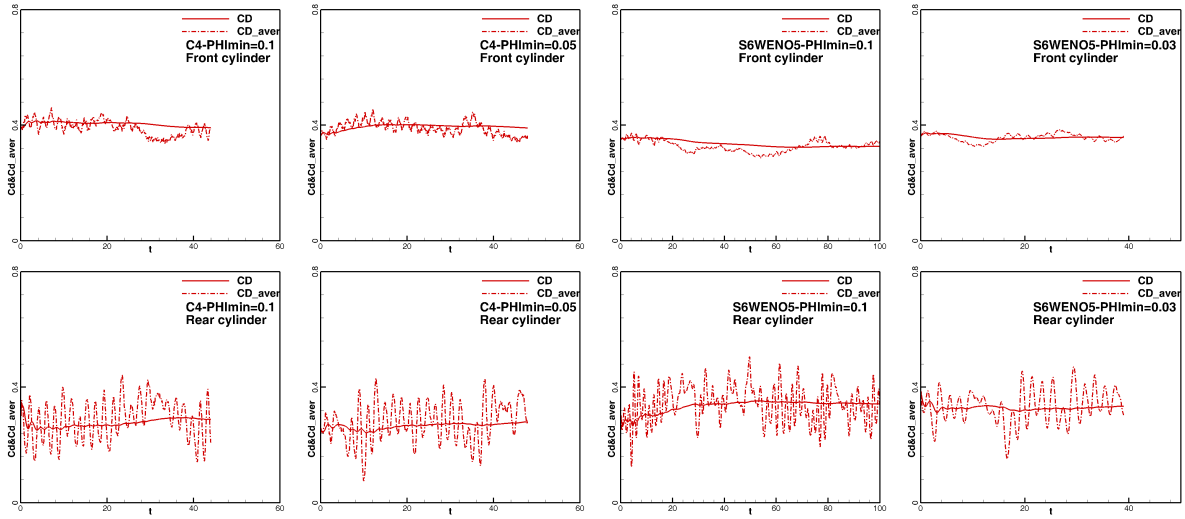

Figure 2. The histories of drag coefficients

Schemes and ϕ_{min}		Averaging time T	Averaged C_D of Front cylinder	Averaged C_D of Rear cylinder
S6WENO5	ϕ_{min}=0.1	100	0.441	0.455
	ϕ_{min}=0.03	41	0.476	0.437
C4	ϕ_{min}=0.1	50	0.522	0.385
	ϕ_{min}=0.05	45	0.520	0.373

Table 1 The comparisons of C_d using different schemes and ϕ_{min}

4.2.2 Effects on Mean Pressure and Root Mean Square Pressure

Figure 3 presents the comparisons of C_p and $C_{p,rms}$ by C4 and S6WENO5 schemes with different ϕ_{min}. The primary difference is not caused by ϕ_{min}, but by the fundamental schemes.

Both C4 and S6WENO5 can well predict the mean C_p on the two cylinders and they differ from each other slightly. C4 presents a little larger suction peaks near 90 and 270 degrees than those of S6WENO5.

After comparing the $C_{p,rms}$,

(1) On the front cylinder: C4 obviously over-predicts the $C_{p,rms}$ than those of the experiments and S6WENO5. S6WENO5 with ϕ_{min} of 0.03 and 0.1 well match the measurements. It seems that S6WENO5 with ϕ_{min} of 0.1 performs better than that with ϕ_{min} of 0.03. The latter ϕ_{min} presents a little smaller $C_{p,rms}$ at about 270 degrees than the measurements.

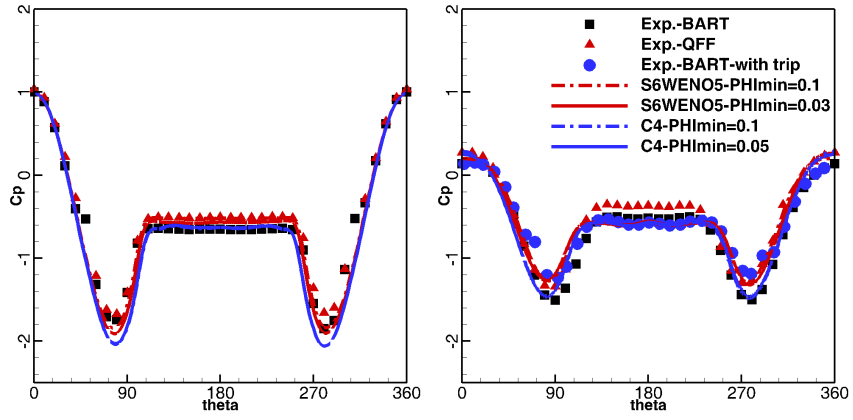

(a) Mean C_p on the cyliners

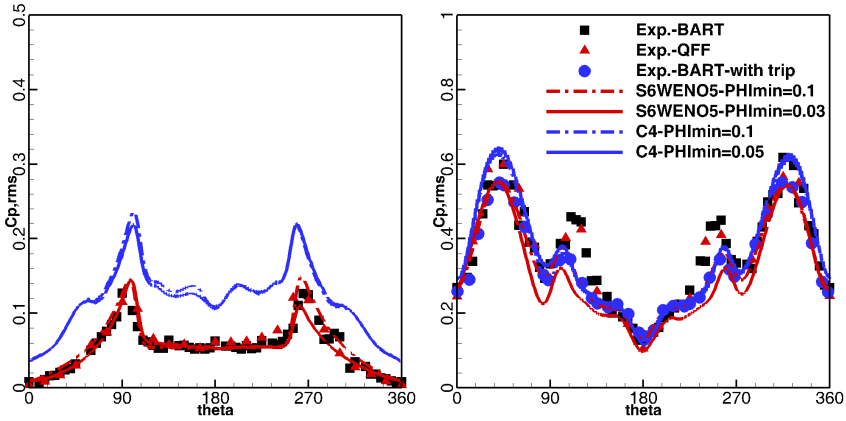

(b) $C_{p,rms}$ on the cylinders

Figure 3. Comparisons of C_p and $C_{p,rms}$

(2) On the rear cylinder: Both C4 and S6WENO5 can well match the measurements, although C4 presents a little larger $C_{p,rms}$ than those of S6WENO5. In S6WENO5 scheme, the large ϕ_{min} performs better than the small one.

4.2.3 Effects on Mean Velocity in Space

Figure 4 presents the comparisons of the mean streamwise velocity by C4 and S6WENO5 with different ϕ_{min}. All the schemes over-predict the recirculation behind the rear cylinder, even comparing with the measurements with trip on the windward surface of the rear cylinder, whose recirculation looks much larger than that without trip.

(1) C4 schemes with ϕ_{min} of 0.1 and 0.05 differ from each other slightly. Both of them under-predict the recirculation in the gap region and over-predict the recirculation in the wake.

(2) S6WENO5 scheme performs better than C4. S6WENO with ϕ_{min} of 0.03 well matches the measurements in the gap region, while it over-predicts the recirculation in the wake. S6WENO5 with ϕ_{min} of 0.1 also over-predicts the recirculation in the gap region but it well matches the recirculation in measurements of BART with trip. Here, larger ϕ_{min} leads to a larger recirculation in the gap region.

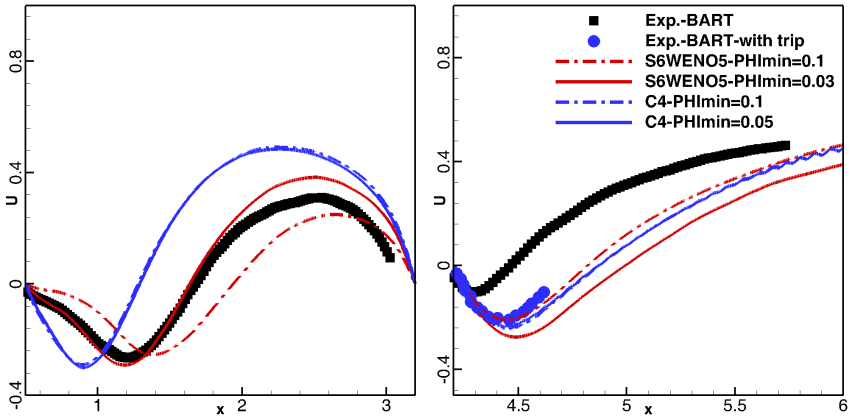

(a) On the central line in the gap and wake

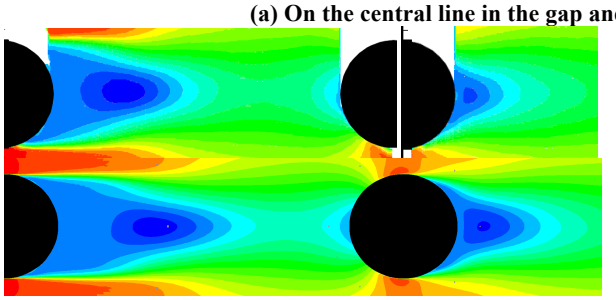

Exp.-BART

S6WENO5-ϕ_{min}=0.1

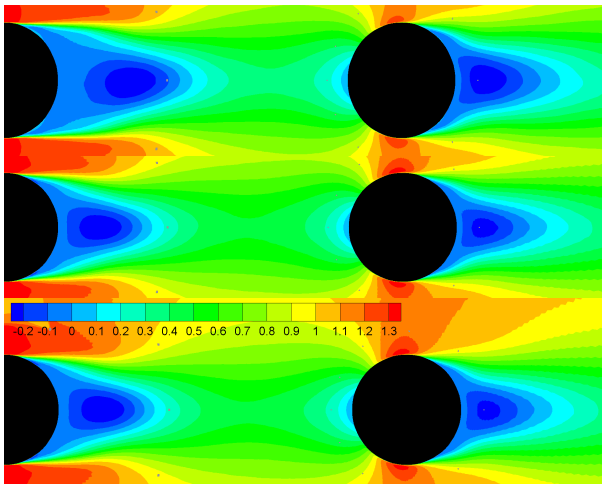

(b) Two-dimensional flowfields

Figure 4 Comparisons on the mean streamwise velocity

4.2.3 Effects on TKE in Space

Figure 5 presents the comparisons of the mean TKE by C4 and S6WENO5 with different ϕ_{min}.

Like the streamwise velocity, C4 with different values of ϕ_{min} perform almost the same.

(1) In the gap region, due to small recirculation, C4 over-predicts the TKE before x/D=1.9, while it under-predicts the TKE after x/D=1.9. In the wake after the rear cylinder, C4 under-predicts the TKE.

(2) C4 scheme with ϕ_{min} of 0.1 predicts a little larger TKE before the peaks and smaller TKE after the peaks than those by C4 with ϕ_{min} of 0.05.

S6WENO5 scheme with two values of ϕ_{min} presents a relatively distinguished difference.

(1) In the gap region, S6WENO5 with ϕ_{min} of 0.03 well matches the measurements before x/D=1.9, while it under-predict the TKE after x/D=1.9. S6WENO5 with ϕ_{min} of 0.1 performs adversely, at another streamwise position of x/D=2.0.

(2) In the wake after the rear cylinder, S6WENO5 schemes with both ϕ_{min} under-predict the TKE.

The same tendency can be reflected in the two-dimensional TKE fields.

(1) In the gap region, the high TKE region is presented a little more upstream by C4 schemes with two ϕ_{min}. The high TKE region by S6WENO5 looks relatively reasonable, but the numerical range of high TKE region looks a little smaller than that of experiment.

(2) In the region of wake after the rear cylinder, the computations differ from the measurements relatively significant. All the schemes under-predict the TKE.

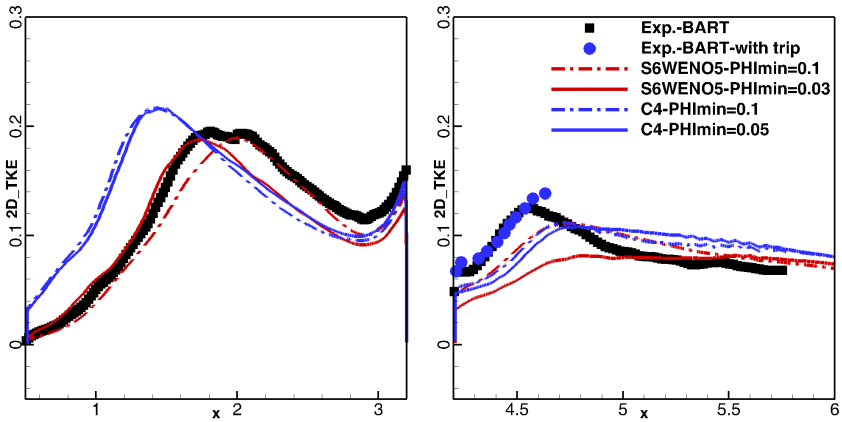

(a) On the central line in the gap and in the wake

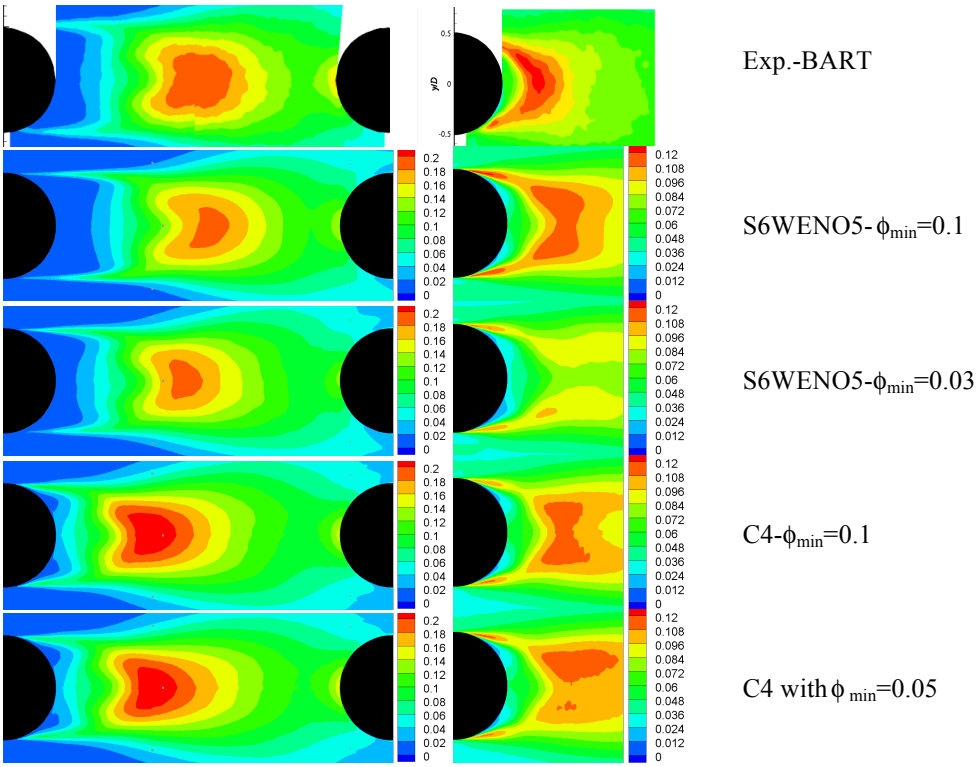

(b) Two-dimensional turbulence flowfields

Figure 5 Comparisons of mean TKE

4.2.4 Effects on Instantaneous Spanwise Vorticity and Q Criterion

In the above sub-sections, the mean and root mean square flow quantities by C4 and S6WENO5 with different ϕ_{min} are compared with the measurements. In this sub-section, the instantaneous flows are presented to demonstrate the performances of the fundamental schemes and different values of ϕ_{min}.

All the numerical schemes coupled with IDDES can resolve the small-scale structures. The primary difference is mainly caused by the fundamental schemes and the ϕ_{min} has a relatively weak influence on the small motions.

The comparisons of spanwise vorticity are presented in Figure 6. The shear layer instability by C4 scheme seems more upstream and the small-scale structures are smaller than those by S6WENO5 scheme. However, some numerical oscillations are demonstrated by C4 with the two values of ϕ_{min}. If ϕ_{min} is smaller, the noise is more obvious. The deficiency of background artificial viscosity ($k^{(4)}$=1/100) is a possible reason, which causes the numerical oscillation. At the same time, the smaller ϕ_{min} is able to cause the shear layer instability a little more upstream.

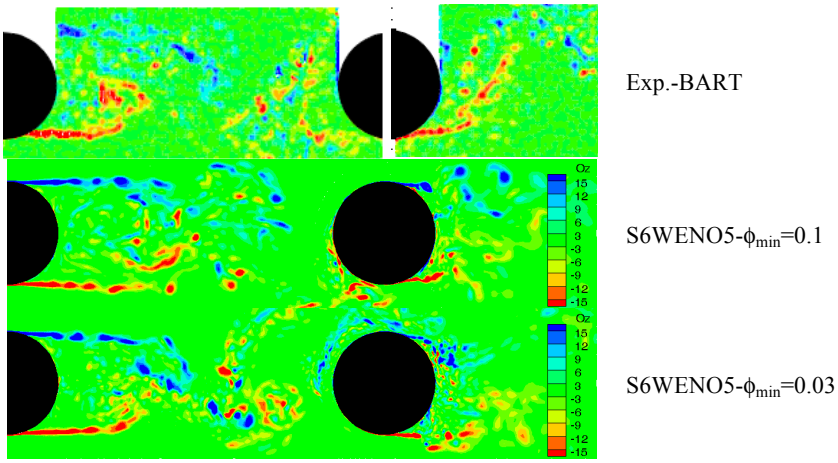

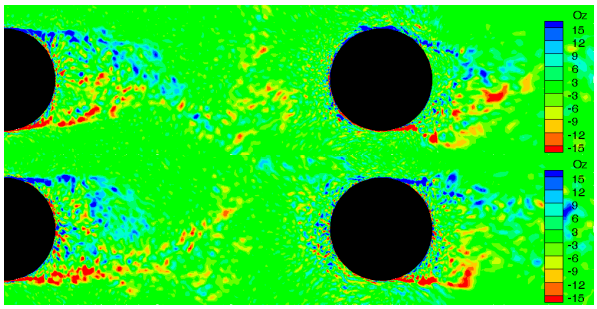

Figure 6 Comparisons of instantaneous spanwise vorticities

The comparisons of instantaneous Q criterion of -5 are demonstrated in Figure 7. All the schemes can well capture the spanwise small-scale structures. Overall, the small-scale structures by C4 scheme are much smaller and more chaotic than those by S6WENO5 scheme.

(1) On the windward side of the front cylinder, C4 scheme with both ϕ_{min} present some very small structures near the windward wall. It indicates that the background artificial viscosity is not enough to suppress the numerical noise.

(2) The performances of both ϕ_{min} based on S6WENO5 scheme are anticipant, where the freestream is very quiet and small-scale structures are presented in the gap and wake region. The structures by the small ϕ_{min} of 0.03 are more and smaller than those by relatively large ϕ_{min} of 0.1.

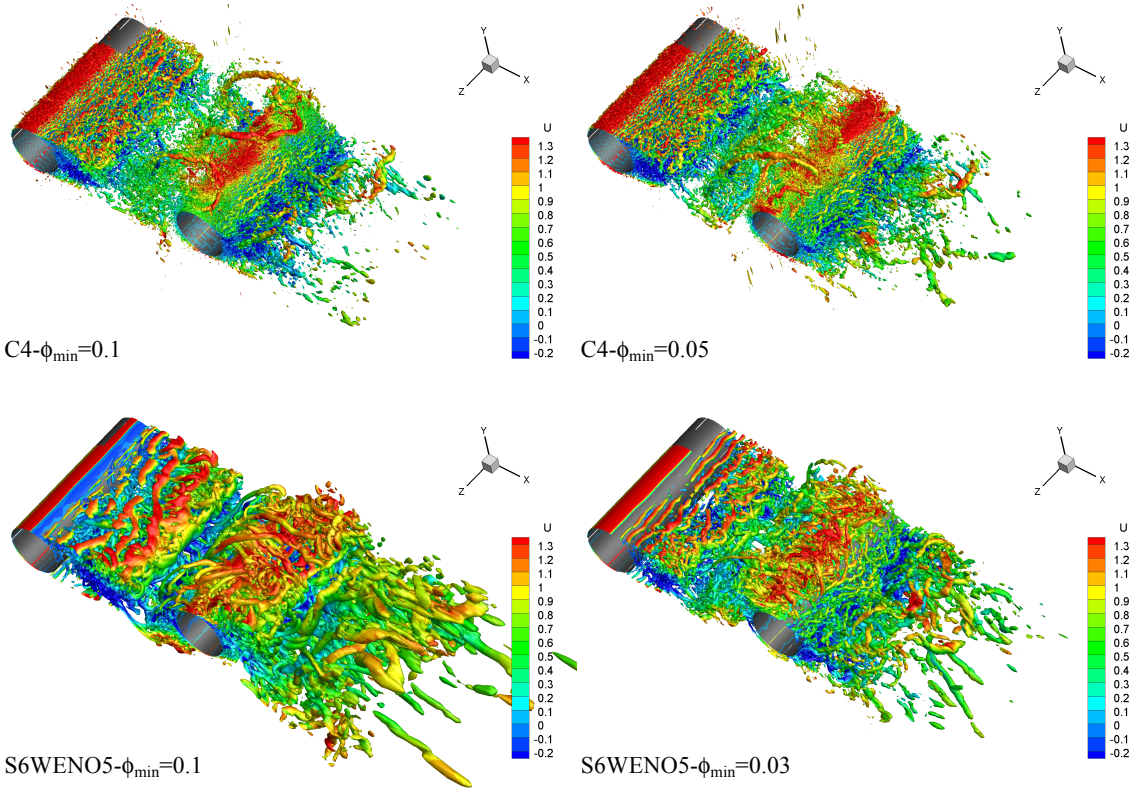

Figure 7 Comparisons of Q criterion

Figure 8 presents the distribution of modeled eddy viscosity and the adaptive function. It is found that the modeled eddy viscosities by C4 and S6WENO5 with different ϕ_{min} look very similar.

(1) C4 scheme: The adaptive function by C4 is possibly affected by the grid scale, because the adaptive function ϕ approaches ϕ_{min}, where the grid scale is small. In addition, the adaptive function ϕ is hoped to be 1 before the front cylinder, where the flow is irrotational. However, an undesired region of adaptive function ϕ, where it is less than 1, is presented. Very small

artificial viscosity before the front cylinder in the irrotational region will lead to the unphysical numerical oscillation in the gap and wake region. The ϕ_{min} has a weak influence on the modeled eddy viscosity and the distribution of adaptive function.

(2) S6WENO5 scheme: The distribution of ϕ is anticipant. In the irrotational region, ϕ approaches to 1 to avoid the numerical oscillation. In the separated region, ϕ approaches to ϕ_{min} to weaken the bad effect of the numerical dissipation on the small-scale motions. However, when is ϕ_{min} small (0.03), the region of ϕ_{min} is over-predicted, which even intrudes the irrotational region.

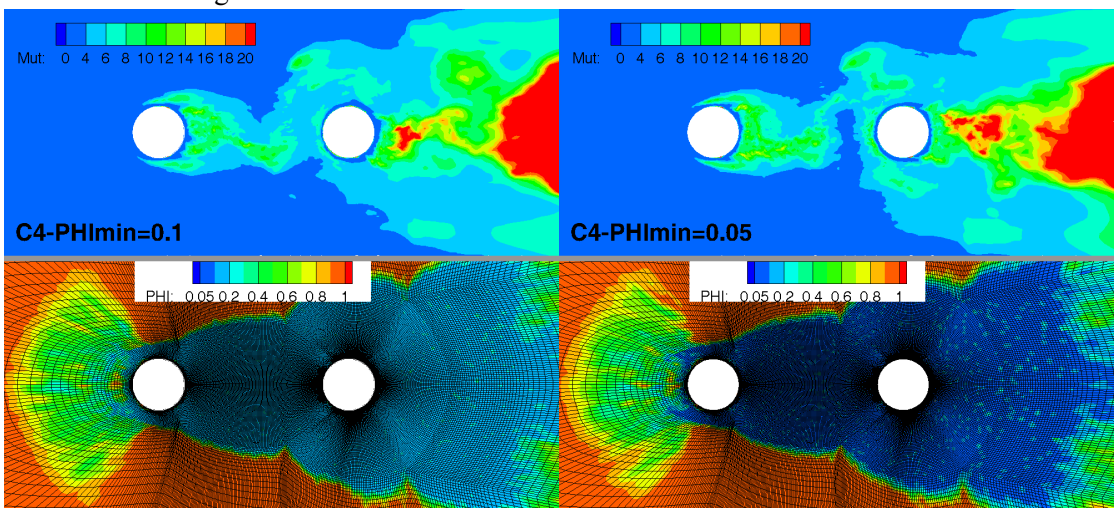

(a) C4 scheme

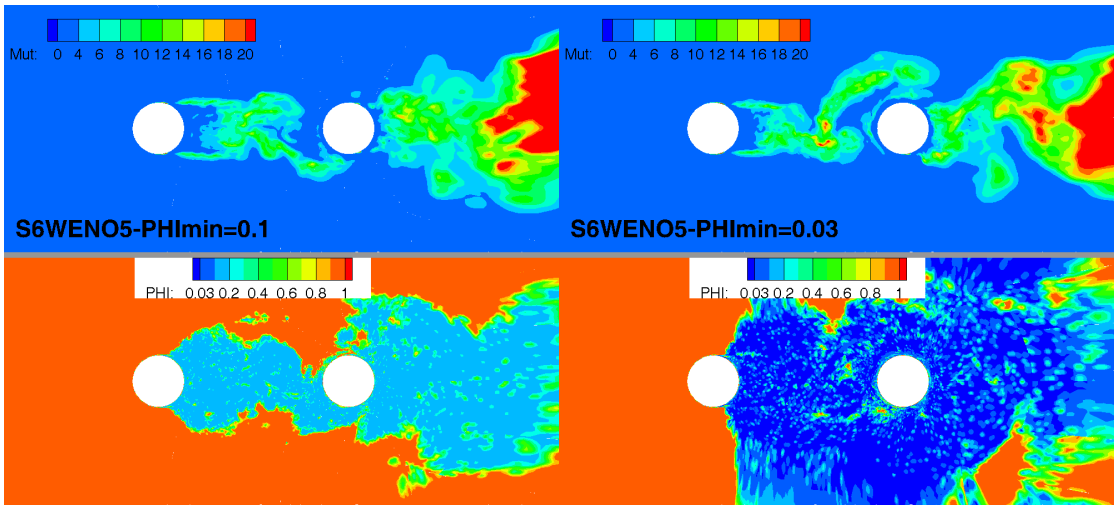

(b) S6WENO5 scheme

Figure 8 Instantaneous modelled eddy viscosity and adaptive function distributions

5 Conclusions and Future Work

The thresholds of adaptive function (ϕ_{min}) in the numerical dissipation for C4 and S6WENO5 schemes, coupled with IDDES based on SST model, are evaluated through DHIT and the massively separated flows past the tandem cylinders.

From the DHIT case, the reasonable choices of ϕ_{min} for C4 and S6WENO4 schemes are recommended after comparing the energy cascade.

After comparing the computations with the available measurements with and without trip, the primary difference of performance is mainly caused by the fundamental schemes, but not ϕ_{min}. Small ϕ_{min} always leads to the shear layer instability a little more upstream. S6WENO5 scheme with two values of ϕ_{min} performs well, and smaller ϕ_{min} presents more and smaller structures in the gap and wake region.

Due to the insufficient background artificial viscosity, C4 scheme with two values of ϕ_{min} demonstrates the numerical oscillations in the instantaneous near-fields, although the mean flows by C4 are very similar with those by S6WENO5 scheme.
Large background artificial viscosity of C4 scheme will be investigated to suppress the numerical oscillation before the front cylinder.

Acknowledgement

This work was partly supported by EU project Advanced Turbulence simulation for Aerodynamic Application Challenges (ATAAC, Contract No. ACP8-GA-2009-233710) and partly by National Science Foundation of China (Grant No. 10932005 and 11072129). The authors thank NTS for the two-dimensional grids in project ATAAC. The authors also thank Shanghai Supercomputer Center (SSC) and Tsinghua National Laboratory for Information Science and Technology for the computational resources.

References

[1] Bui T.T., "A Parallel, Finite-Volume Algorithm for Large-Eddy Simulation of Turbulent Flows," NASA/ TM-1999-206570, 1999.

[2] Jameson A., Schmidt W. and Turkel E., "Numerical Solutions of Euler Equations by Finite Volume Methods with Runge-Kutta Time Stepping Schemes," AIAA Paper 1981-1259, 1981.

[3] Menter F.R., "Two-Equation Eddy-Viscosity Turbulence Models for Engineering Applications," AIAA J. 32(8), pp.1598-1605, 1994.

[4] Menter F.R. and Kuntz M., "A Zonal SST-DES Formulation," DES WORKSHOP, St. Petersburg, Russia, July 2003, (http://cfd.me. umist.ac.uk/flomania/index2.html) [retrieved 26 Feb. 2012].

[5] Mockett, C., "A Comprehensive Study of Detached-Eddy Simulation," Doctoral thesis, Technical University Berlin, 2009.

[6] Neuhart D.H., Jenkins L.N., Choudhari M.M. and Khorrami M. R., "Measurements of the Flowfield Interaction Between Tandem Cylinders," AIAA Paper 2009-3275, 2009.

[7] Qin N. and Xia H., "Detached Eddy Simulation of a Synthetic Jet for Flow Control," Proceedings of the Institution of Mechanical Engineers, Part I: Journal of Systems and Control Engineering, 222(5), pp. 373-380, 2008.

[8] Shur M.L., Spalart P.R., Strelets M. and Travin A., "A Hybrid RANS-LES Approach with Delayed-DES and Wall-Modelled LES Capabilities," Int. J. Heat Fluid Flow. 29, pp.1638-1649, 2008.

[9] Spalart P.R. and Allmaras S.R., "A One-Equation Turbulence Model for Aerodynamic Flows," AIAA paper 92-0439, 1992.

[10] Spalart P.R., Jou W.H., Strelets M. and Allmaras S.R., "Comments on the feasibility of LES forwings, and on a hybrid RANS/LES approach," First AFOSR International Conferenceon DNS/LES, Ruston, LA. Advanced in DNS/LES.GreydenPress, Columbus, OH, 1997.

[11] Spalart P.R., Deck S., Shur M., Squares K., Strelets M. and Travin A., "A New Version of Detached Eddy Simulation, Resistant to Ambiguous Grid Densities," Theoretical and Computational Fluid Dynamics, 20(3), pp. 181–195, 2006.

[12] Spalart P.R., Shur M.L., Strelets M.K. and Travin A.K., "Sensitivity of Landing Gear Noise Predictions by Large Eddy Simualtion to Numerics and Resolution," AIAA paper 2012-1174, 2012.

[13] Strelets, M., "Detached Eddy Simulation of Massively Separated Flows," AIAA paper 2001-0879, 2001.

[14] Usta E., "Application of a Symmetric Total Variation Diminishing Scheme to Aerodynamic of Rotors," Doctor thesis, Georgia Institute of Technology, 2002.

[15] Xiao Z.X., Liu J., Huang J.B. and Fu S., "Comparisons of Three Improved DES Methods on Unsteady Fows past Tandem Cylinders. 4th Symposium on RANS/LES Hybrid Methods. Beijing, 28-30, Sep., 2011

[16] Xiao Z.X., Liu J., Huang J.B. and Fu S., "Numerical Dissipation Effects on the Massive Separation around Tandem Cylinders. AIAA Journal, 55(5), pp. 1119-1136, 2012.

[17] Xiao Z.X., Liu J., Luo K.Y., Huang J.B. and Fu S., "Numerical Investigation of Massively Separated Flows past Rudimentary Landing Gear Using Advanced DES Approaches", AIAA Journal, (accepted).